



**POLITECNICO**  
MILANO 1863

SCUOLA DI INGEGNERIA INDUSTRIALE  
E DELL'INFORMAZIONE



**von KARMAN INSTITUTE**  
**FOR FLUID DYNAMICS**

EXECUTIVE SUMMARY OF THE THESIS

## Inter refrigerated compression through stator cooling

LAUREA MAGISTRALE IN MECHANICAL ENGINEERING - INGEGNERIA MECCANICA

**Author:** STEFANO PLATINI

**Advisor:** PROF. PAOLO GAETANI

**Co-advisor:** FABRIZIO FONTANETO, BOGDAN CERNAT

**Academic year:** 2021-2022

### 1. Introduction

The research on new technologies to reduce the carbon emission is engineers' challenge of today. The European project Alliance for Zero-Emission Aviation and the WINGS one (Wallon INnovations for Green Skies) of the Wallonie government aim to join forces in preparing for the advent of zero-emission aircraft. The use of hydrogen as fuel is a possible solution to face this challenge: some automotive land applications are already entering the market. The liquid state is necessary to store a fuel quantity sufficient for all the flight envelope and it can be obtained only with low temperature or high pressure, higher than the combustion chamber one. Both conditions create a free heat sinking ( $\nabla T$  or  $\nabla P$ ) that could be exploited to cool down the fluid. This thesis project aims to investigate the effect of an inter refrigerated compression on the efficiency value of a Joule Brayton cycle compared to an adiabatic one. The advantages will be of 1 – 2 point percentage due to the inter refrigerated compression and up to 4 – 5 point percentage considering also preheating of fuel due to regeneration. To keep the same weight and design of the aeroengine, the heat transfer process could be performed using the stator blade as cooler. The stator blade is designed to satisfy the aerodynamic machine requirements and not to exchange heat: the *CFD*

analysis on a known compressor stage, *DREAM* (from the European project [1]), allows to estimate the heat transfer coefficient of the surface and to quantify the amount of heat that could be extracted. The final study regards the coupling of the results to quantify the possible real advantages of this configuration.

### 2. Joule-Brayton cycle analysis

To set the CFD boundary conditions and to understand the cooling position which gives the best results in terms of efficiency, a 1D thermodynamic analysis of the cycle is performed numerically with *Matlab2022a*. The code simplifies the Joule Brayton cycle in 7 steps:

- Fan compression ( $\beta_{fan}$ )
- Low pressure compression(LPC)
- Inter refrigeration
- High pressure compression (HPC)
- Combustion
- High pressure turbine (HPT)
- Low pressure turbine (LPT)

The code analyses 2 real engines in both take off and cruise condition: CFM56-7B24 used for short-mid range application and GENX-1B64 applied for long run application. The real parameters of these machines (mass flow, inlet condition, outlet condition, fan compression ratio, bypass ratio) are used as input in the thermodynamic code. The amount of heat extracted

with inter refrigeration and the position at which cooling happens are the free variables that create an efficiency matrix. The amount of heat is estimated through the  $q^*$  parameter as a ratio (from 0 to 1) of the total enthalpy increase due to the LPC.

## 2.1. Inter refrigerated cycle

The cycle is studied for all the applications with a fixed power input, a fixed quantity of fuel injected, or with a fixed turbine entry temperature: both the approaches can be used and the second one is chosen to keep the global pressure ratio of the engine constant at cruise and takeoff condition. There is a combination of pressure ratio and turbine entry temperature which maximises the efficiency of a Joule-Brayton cycle[3]. The optimal results for a turbine entry temperature of 2200 K are reported in Table 1.

	CFM		GENX	
	Cruise	Takeoff	Cruise	Takeoff
$\eta_{max}$	0.4833	0.4573	0.53151	0.5269
$\beta_{cooling}$	1.9564	2.1303	1.6955	1.7173
$\Delta\eta$	1.73 %	1.82%	1.27%	1.12%
$q^*$	1	1	1	1
$Q[MW]$	1.3	3.32	2.16	5.2

Table 1: Optimal results for  $T_{turbine}$  of 2200K

The results show an optimal position of the inter refrigeration in the booster compressor and a  $q^*$  value equal to 1. The new optimal cycle for GENX engine at takeoff condition is in Figure 1.

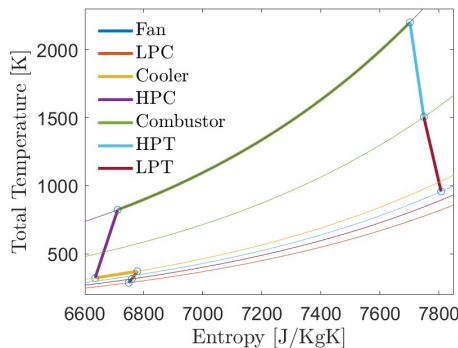


Figure 1: Thermodynamic optimal cycle for GENX takeoff

The results of the other machines are similar and the optimal cooling position is always in the booster compressor. The work produced by

the turbine is fixed with the turbine entry temperature and the outlet pressure ratio. The results of the optimal position can be explained with the reduction of work in the HPC due to cooling, the combination of LPC and HPC work required to reach the global compression ratio and the increase of fuel consumption with the amount of heat removed. These results create the boundary condition for the CFD analysis on the booster compressor DREAM, a LPC in the Von Karman Institute R-4 facility, studied for its capability of reducing of flow distortions [5].

## 2.2. Inter refrigerated and regenerated cycle

In subsection 2.1 the heat extracted is considered lost in the thermodynamic state transformation, in the metal structure or in the pressure losses due to the small channel. The double function of hydrogen, used both as coolant and as fuel, allows to perform a regeneration of the cycle. The regeneration usually exploits the heat of the flow downstream the LPT to heat up the fuel to increase its chemical energy. In this application the heat is taken from the LPC and allows a reduction of the amount of fuel injected to reach the same turbine entry temperature. The increase of efficiency due to regeneration is reported in Figure 2: the light blue bar is the adiabatic  $\eta$ , the orange is the increase with inter refrigeration only and the yellow is the further beneficial effect of coupling inter refrigeration and regeneration through preheating of the fuel.

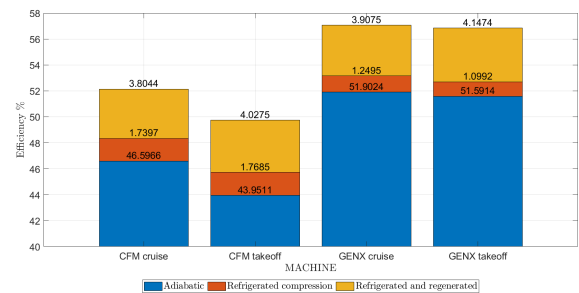


Figure 2:  $\Delta\eta$  due to inter cooling (orange) and regeneration(yellow)

The amount of heat extracted in the optimal regenerated cycle, normalized with the heat injected with the fuel, is comparable to the increase of cycle efficiency. This effect changes the optimal position of the cooled stage increasing

the compression ratio and, with the same optimal  $q^*$  parameter ( $q^* = 1$ ), the amount of heat removed. The new optimal cycle for the GENX engine at cruise condition is visible in Figure 3.

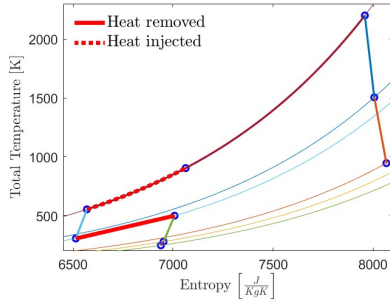


Figure 3: Joule Brayton cycle with regeneration

The heat removed with cooling (red continue line) is injected in the combustion chamber (red dotted line) and it reduces the  $\Delta h_t$  required to the fuel to reach a turbine entry temperature of 2200K. The results for the four engines are summarised in Table 2.

	CFM		GENX	
	Cruise	Takeoff	Cruise	Takeoff
$\eta_{max}$	0.5214	0.4975	0.5706	0.5684
$\beta_{cooling}$	6.1616	5.2759	6.3023	5.9367
$\Delta\eta$	5.85%	6.17%	5.54%	5.68%

Table 2: Optimal inter refrigerated and regenerated cycle

The optimal cooling position for an inter refrigerated and regenerated cycle is in the HPC. The limited possibility of removing such a high quantity of heat through a compressor stage, the real behaviour of heat transfer process with the losses and the topic of this thesis, the inter refrigeration compression only, set the CFD analysis on a booster compressor. The flow through DREAM, a booster compressor stage studied in the VKI facility, is analysed with a cooled stator blade.

### 3. CFD simulation

A CFD study is performed to investigate the heat extraction capability of a stator compressor blade. The studied stage is a booster compressor (DREAM), a high loaded compressor stage in the R-4 Von Karman institute facility, which has been already studied with a numerical model [5]. The numerical analysis of a booster stage in-

stead of a HPC is due to the unknown value of a real possible heat transfer effectiveness, decreasing the amount of heat that reaches the combustor; the  $\Delta\eta$  due to regeneration decreases while the advantages of inter refrigerated only cycle are not affected by heat losses.

#### 3.1. Simulation layout

The simulations run with *Numeca fine turbo 16.1*. The domain spatial discretisation comes from the ASME article one [5]. The original mesh is modified with *IGG 16.1*, the built in grid generator of *Numeca* in the module *Auto-Grid*. The new mesh has the default topology (*O4H*) and allows faster and cheaper simulations: the cell number is reduced from 64 to 2.2 millions. The blade to blade domain at 50% of span is visible in Figure 4.

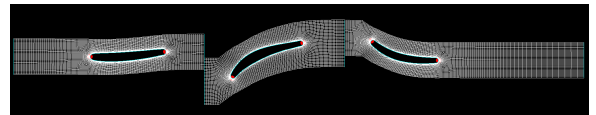


Figure 4: Mesh view: B2B at 50% span

The results of subsection 2.1 do not show a flight envelope status in which the inter refrigeration can be more effective and so there is not a specific boundary condition that should be applied to simulate it. The 5 boundary conditions required are applied both at inlet section(4) and at outlet section(1). At inlet the experimental  $T_T$  and  $P_T$  profiles are imposed with a surface normal velocity direction. The outlet condition is the designed mass flow ( $11.442 \frac{Kg}{s}$ ) with pressure adaptation condition to stabilise the simulation. The solid boundary conditions in turbomachine simulations are usually imposed adiabatic: this decision is due to the lack of data related to the metal temperature and due to the high quantity of work exchange between the fluid and the machine respect with the amount of heat is negligible. The optimisation process applied to turbomachine is starting considering also the heat transfer process and there are some publications regarding how it affects the CFD results [2]. A fixed metal temperature is applied on stator blade surface to simulate an internal cooling. The estimation of a heat transfer coefficient  $h$  [ $\frac{W}{m^2 \cdot K}$ ] requires different temperatures and the adiabatic case is compared to a fixed metal temperature of 300K, 290K and 280K. The bound-

ary layer is simulated with the  $k-\omega SST$  model. The turbulence sensitivity analysis, reported in the ASME article [5], shows no effects of turbulent model at design condition and it is assumed valid also in this case. A comparison between the  $k-\omega SST$  and the Spalart Allmaras (SA) turbulence model is done and confirms this trend. The flow is solved with 2 steps of multi grid level and all the simulation reaches convergence with a global residual between  $-5.75$  and  $-5.78$ . The number of iteration is 2500 for the coarser levels and 5000 for the finest one.

### 3.2. Simulation results

The simulations reach convergence and the reduction of the global residual is sufficient to thrust the results. The stage efficiency increases with the reduction of the stator metal temperature. This is a fictitious effect of cooling due to the efficiency definition in case of a compressor stage: the efficiency is reported in the *Numeca User Guide* [4] and in Equation 1

$$\eta_{is} = \frac{\left(\frac{p_{t2}}{p_{t1}}\right)^{\frac{\gamma-1}{\gamma}} - 1}{\frac{T_{t2}}{T_{t1}} - 1} \quad (1)$$

The  $P_T$  profile of the four simulations (adiabatic,  $T_{stator} = 300K, 290K, 280K$ ) are comparable and the increase of efficiency is due to the reduction of the  $T_{T2}$  value at the stage outlet. The built in definition of efficiency does not take into account the heat losses which are forced by the cooling of the blade. The quantity used to estimate the amount of heat extracted through the stator blade is the total enthalpy ( $h_T$ ); the difference between the  $h_T$  of the cooled stage and the adiabatic one is the heat removed with cooling. This  $h_T$  quantity is a scalar value obtained through the surface integral of the outlet section which stays 2.5 chords after the stator trailing edge. The scalar integral operation is a built in function of the *Numeca* post processor *CFView*. The results for the different stator temperature, with different turbulence models, are summarised in Table 3.

	$T_s 300K$	$T_s 290K$	$T_s 280K$
$Q \left[\frac{J}{kg}\right]$	161.19	301.17	445.39
$Q SA \left[\frac{J}{kg}\right]$	182.40	332.98	489.93

Table 3: Heat extraction comparison  $K-\omega SST$  and SA

The amount of heat extracted is not comparable to the optimal one of subsection 2.1, there are two orders of magnitude between the cycle results (MW of heat removed) and the heat removed through the DREAM stator blade ( $500 \frac{J}{Kg} \cdot 11.442 \frac{Kg}{s} \sim 10KW$ ). The SA turbulence model gives better results in terms of heat exchange through the blade. The heat transfer coefficient is the slope of the curve. Between the two models there is a small variation and  $h$  value can be estimated as average to a value of  $80 \frac{KW}{m^2K}$ . The effect of a fixed temperature boundary condition in the flow channel is estimated comparing the  $h_T$  values to the ones on a secondary surface which is  $\frac{1}{4}$  chord far from the stator trailing edge. The  $h_T$  maps for the adiabatic case and the 280K simulation are in Figure 5.

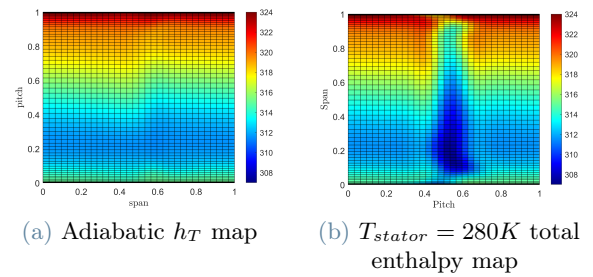


Figure 5: Secondary surface at  $\frac{1}{4}$  chord distance away from stator trailing edge:  $h_T$  values

The cooling effect is visible in the deep blue region in the center of channel. Summing the  $\Delta h_T$  spanwise and pitchwise, Figure 6, some considerations can be done on how the cooled surface affects the flow:

- The effect of a cooled surface in the middle of flow channel is clearly visible pitchwise
- The variation of enthalpy does not affect the global pitch of the channel
- The end wall has a high capacity of heat extraction due to higher level of turbulence.

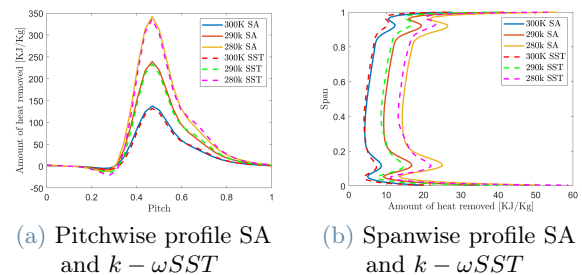


Figure 6:  $\Delta h_T$  profiles pitchwise and spanwise

This considerations lead to the analysis of three other possible configurations to increase the amount of heat extracted with a stator blade.

### 3.3. Layout variation

The possible layout variations to increase the amount of heat extracted are:

- Cooling the casing only
- Cooling the casing and the stator blade
- Increasing the solidity with blade numbers

#### 3.3.1 Cooling casing only

Figure 6b shows a higher heat exchange process at the endwall than the free stream one due to the boundary layer development. To investigate the amount of heat extraction of the casing only, the simulations run with a fixed  $T_T$  condition on the casing surface. An internal cooling of the casing will be easier to realize instead of the stator blade one due to the higher thickness available which allows easily placing of the coolant pipes. The casing surface is lower than the blade one but the amount of heat removed in terms of  $\frac{J}{Kg}$  is comparable: Table 4 shows it.

	$T_s 300K$	$T_s 290K$	$T_s 280K$
$Q_{basecase} [\frac{J}{kg}]$	161.19	301.17	445.39
Q only casing $[\frac{J}{kg}]$	182.40	271.48	358.43

Table 4: Heat extraction comparison

The cooling of casing only creates a significant total temperature gradient in the spanwise direction and this leads to a variation of the work done in the different stream lines: this effect has to be considered in the final machine design.

#### 3.3.2 Increasing of solidity

Another layout variation to increase the amount of heat extracted is to increase the solidity through the blade numbers. The internal blade cooling affects the flow in pitch direction between 0.38 and 1 as it is visible in Figure 6a. The number of stator blades is increased from 100 to 144 to reduce the pitch, this leads to an increase of the machine weight too but also allows a higher load and a reduction in the number of stages. This consideration should be considered during the future engine design. The amount of heat extracted per unit of mass increases due

to an increase of the heat exchange surface area (Table 5).

	$T_s 300K$	$T_s 290K$	$T_s 280K$
$Q_{basecase} [\frac{J}{kg}]$	161.19	301.17	445.39
Q 144 blades $[\frac{J}{kg}]$	485.6	812.4	1142.2

Table 5: Heat extraction comparison with different solidity

The variation of  $h_T$  pitchwise does not change from the base case with 100 stator blades. This result means that, reducing the pitch dimension, the percentage of flow affected by cooling remains the same. The reason of this behaviour is in the boundary layer development: all the simulations run with a design mass flow and the pressure gradient blade to blade remains the same. The decreasing of load decreases the Re number and the flow becomes more laminar. The reduction of turbulence compensates the reduction of pitch and the amount of flow affected by cooling remains the same.

#### 3.3.3 Cooling casing and blade

The internal coolant channels have to pass through the casing to reach the stator blade and the casing will be cooled too. The amount of heat extracted imposing a fixed total metal temperature both to casing and blade is in Table 6.

	$T_s 300K$	$T_s 290K$	$T_s 280K$
Q blade+casing $[\frac{J}{kg}]$	337.22	564.16	793.22

Table 6: Heat extraction cooling casing and blade surface

A final graphical comparison of all the cases studied can be seen in Figure 7.

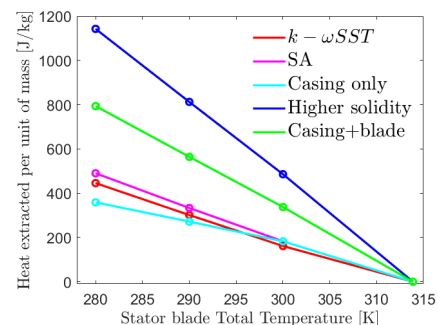


Figure 7: Comparison of simulations



## 4. Joule Brayton numerical cycle with CFD results

The CFD analysis quantifies a limited capability in the heat extraction process available cooling a LPC stator blade. This results is obtained with a fixed  $T_T$  imposed on all the blade surface and it will overestimate the real capability of an internal cooling. The numerical analysis of a Joule Brayton cycle with an inter refrigerated compressor stage, able to extract a fixed quantity of heat (from CFD results), gives the following efficiency map (Figure 8) in case of  $T_{stator} = 280K$ .

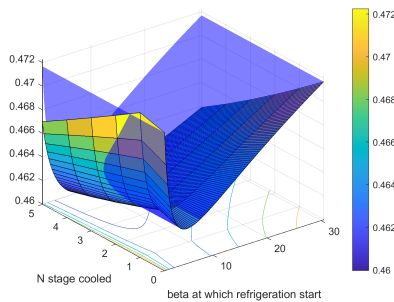


Figure 8: Efficiency comparison of an inter refrigerated (colored) and adiabatic (blue) cycle of CFM engine at cruise condition

The map shows the efficiency value of an inter refrigerate (colored) Joule Brayton cycle compared to the adiabatic one (blue curve), function of the cooling position and of the amount of refrigerated stages, from 1 to 5. The results of the four machines analysed are summarised in Table 7. The  $\beta_{cooling}$  and the  $N_{stages}^o$  cooled are equal to "1" in all the simulations.

	CFM		GENX	
	cruise	take-off	cruise	take-off
$\eta$	0.4722	0.4456	0.5240	0.5206
$\Delta\eta$	0.057%	0.058%	0.053%	0.053%

Table 7: Results with a stator temperature of  $280K$ :  $405 \frac{J}{Kg}$  removed per stage

## 5. Conclusions

The objectives of this thesis are to study the effects of an inter refrigerated compression process in the Joule Brayton cycle and to estimate heat transfer coefficient for a stator blade. The results of the numerical cycle analysis set the optimal cooling position in the booster, in case of an inter refrigerated compression only, or at

the beginning of the HPC in case of inter refrigerated and regenerated cycle with a unitary heat transfer effectiveness. The estimated efficiency advantages are very relevant and they could lead to a higher investment in the development of zero emission aeronautics engine filled with hydrogen. The CFD study, performed on the booster DREAM, gives an estimation of the heat transfer coefficient  $h$  to the value of  $80 \frac{KW}{m^2K}$  for the blade surface. This coefficient does not allow the extraction of the optimal amount of heat from the cycle point of view and the cooling position, which maximises efficiency, goes after the fan. The efficiency advantage due to a limited amount of cooling available reaches, in case of cooling applied both to blade and casing, the order of one tenth of a percentage point for all the applications. This value is significant in the current aeroengine market. The future developments required by this technology are many, the feasibility of the internal pipes in a compressor blade, the quantification of pressure losses of coolant in the pipes and how they affect the state of hydrogen, the heat losses in the heat exchange process. The European project (AZEPA) and the Belgian one (WINGS) have the objective to realise a zero emission aviation engine by 2050. This work shows and quantifies technological advantages in using hydrogen as coolant before injecting it in the combustor chamber and it would increase the effort on this research topic.

## References

- [1] European Commission. validation of radical engine architecture systems, 2019.
- [2] N.J. Kormanik III. Quantifying heat transfer effects of a high speed, multi stage, axial research compressor, 12 2021.
- [3] Dr. Joachim Kurzke. Aero-engine design: From state of the art turbofans towards innovative architectures: Preliminary design. 2013. VKI lecture series April 9-12,2013.
- [4] Numeca. *User Guide:FINE<sup>TM</sup> Turbo 13.2*. 2013.
- [5] Koen Hillewaert Riccardo Toracchio, Fabrizio Fontaneto. On the impact of the turbulence model on the secondary flow structure of a highly-loaded compressor stage. 2022.